

An Adaptive Kernel Estimation For Blur Removal In License Plate Images Of Fast Moving Vehicles

¹ K.Vineesha, ² SK.Shaguftha

¹PG scholar, Dept. of ECE, Narayana Engineering College, Nellore, India.

² Assistant Professor, Dept. of ECE, Narayana Engineering College, Nellore, India.

Abstract: As the unique identification of a vehicle, tag is a key hint to reveal over-speed vehicles or the ones engaged with attempt at manslaughter mischances. Be that as it may, the depiction of over-speed vehicle caught by observation camera is much of the time obscured because of quick movement, which is even unrecognizable by human. Those watched plate pictures are for the most part in low determination and endure serious loss of edge data, which cast awesome test to existing visually impaired deblurring strategies. For tag picture obscuring caused by quick movement, the obscure portion can be seen as linear uniform convolution and parametrically demonstrated with point and length. In this paper, a novel is proposed plan in view of meager portrayal to distinguish the obscure bit. By examining the inadequate portrayal coefficients of the recuperated picture, To decide the point of the piece in view of the perception that the recouped picture has the most meager portrayal when the bit edge compares to the certifiable movement edge. At that point, This appraise is the length of the movement portion with Radon change in Fourier domain. This plan can well deal with expansive movement obscure notwithstanding when the tag is unrecognizable by human. This assess will be approach on certifiable pictures and contrast and a few prevalent best in class daze picture deblurring algorithms. Test comes about show the predominance of the proposed approach regarding effectiveness and robustness.

Index Terms—Kernel parameter estimation, license plate deblurring, linear motion blur, sparse representation.

I. INTRODUCTION

Tag is the unique ID of every vehicle and assumes a critical part in a bad position creator vehicle. These days, there are heaps of auto over-speed location and catch frameworks for traffic violation on the primary streets of urban areas and high-ways. In any case, the movement of vehicle amid the exposure time would cause the obscure of snapshot image. In this manner, the exposure time (screen speed) has noteworthy effect on the measure of obscure. For video shooting, the exposure time is to a great extent subject to the enlightenment circumstances. In common open air scene with daylight, the commonplace exposure time is around 1/300 second. For a vehicle running at 60 miles perhour,

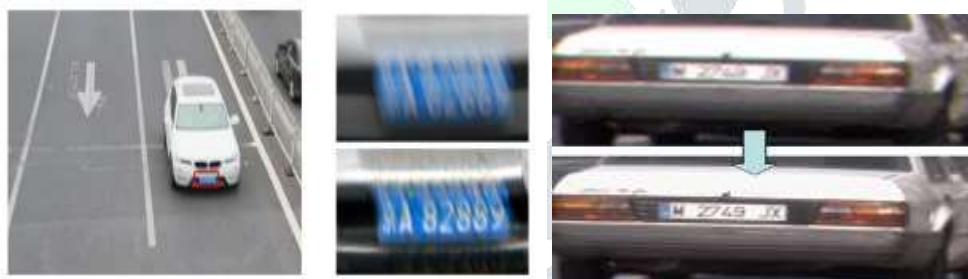


Fig:1 One example of fast-moving vehicle image and our final deblurred result.

amid the exposure time, the displacement of tag is around 9 centimeters which is practically identical with the measure of the tag (14 × 44 centimeters in China), i.e., the length of bit is around 45 pixels when the tag image is with size of 140×440 pixels and the edge between camera imaging plane and flat plane is around 60 degree. In such a situation, the obscure of tag can't be disregarded^[1-3]. In a perfect situation with sound enlightenment, the obscure from shorter exposure time, say, 1/1000 second, can be minor and may not harm the semantic data. In this situation, the principal undertaking of tag deblurring is to recuperate the helpful semantic hint for identification. For instance, for an obscured snapshot of over-speed vehicle, the most imperative issue is to perceive its tag after image deblurring. In the most recent decades daze image deblurring/deconvolution (BID) has picked up bunches of consideration from the image handling group. Albeit a few advances have been made, it is still extremely difficult to address some certifiable cases. Scientifically, the model of image obscuring can be detailed as:

$$B(x,y) = (k * I)(x, y) + G(x, y) \dots (1)$$

where B, I, and k indicate the obscured image, the sharp image we mean to recoup, and the obscure portion, separately; G is the added substance commotion (generally viewed as white Gaussian clamor); and * signifies convolution administrator.

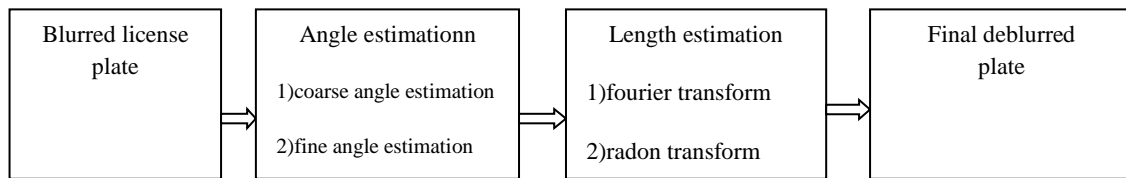


Fig:2 Flow chart of the proposed method

As of late, numerous compelling BID algorithms have been proposed. Because of the not well postured nature of BID, earlier learning is typically acquainted with abstain from falling into the mistaken arrangements^[4-5]. The greater part of them at the same time evaluate portion from the obscured image and apply a non-daze image deblurring (NBID) calculation recursively to approach the genuine arrangement . Given a linear bit $k\theta,l$, a comparing deblurred image $\hat{I}\theta,l$ can be acquired by applying NBID on the obscured image B with $k\theta,l$. At that point the inadequate portrayal coefficients of $\hat{I}\theta,l$ on pre-prepared word reference can be meant as $A(\theta, l)$, which is an element of θ and l . We watch that $A(\theta, l)$ indicates exceptionally valuable semi arched trademark under a settled l . By using this intriguing trademark, we can construe the genuine point of the obscure portion productively^[6-10]. Once the point is resolved, on the course parallel to the movement, the power range of obscured image is clearly influenced by the linear portion in light of which the range is a sinc-like capacity, and the separation between its two nearby zero-intersections in frequency domain is controlled by the length of bit.

II.AFFILIATED WORK

From the perspective of Bayesian acceptance, there are two essential alternatives for BID: most extreme a posteriori (MAP) procedures and underestimation techniques. Of course, for specific piece, the recuperation can be lessened to a parameter estimation issue. In this portion, we will overview a couple of delegate BID plots in the more than three classes.

2.1 MAP approach

The MAP methods attempt to obtain the latent image by solving the following optimization problem:

$$(k,i)=\operatorname{argmax}_{k,i}\{p(k,I|B)\propto p(B|k,I)p(k)p(I)\} \dots\dots(2)$$

where $p(B|k, I)$ is the probability thing which is normally demonstrated with a Gaussian conveyance; $p(k)$ and $p(I)$ mean the earlier learning of part and idle image, separately. As Levin et al. called attention to, the arrangement of innocent MAP system with inclination sparsity earlier normally does not really relate to the bit and sharp image, yet prompts the outcome supporting the "no obscure" arrangement ($\hat{I} = B$). To abstain from acquiring a "no obscure" arrangement, a few preprocessing techniques have been proposed for the MAP system. Shan et al. ^[11]



Fig:3 Images used in our simulation experiment, (a) lena ;(b) sharp image plate

presented another model of spatially irregular appropriation of image commotion and another smooth requirement of idle image. In the creators proposed to include one forecast (or choice) advance to upgrade the extensive scale edges to enhance the execution. In light of a similar thought, Xu et al. presented an unnatural ℓ_0 sparsity earlier, and the sparsity work utilized as a part of their calculation has the comparable impact with edge forecast. In this methodology, the edge expectation is basic for the deblurring execution. Another option is to present more entangled earlier, for example, framelet^[12-13] and straightforwardness data

2.2 Underestimation approach

The minimization strategies depend on the perception that augmenting $p(k|B)$ for the most part prompts a more robust and precise piece even under a frail earlier of sharp image .These strategies right off the bat evaluate the piece by desire expansion (EM) calculation, and after that apply NBID just once. Wang et al. ^[14] consolidated the underestimation strategy and huge scale step edge forecast procedure to enhance the robustness of deblurring calculation. Be that as it may, it can be demonstrated hypothetically that the maxmarginalization strategy can just deal with little portion circumstances (i.e., the measure of bit is substantially littler than the span of watched image). Actually, in our situation, the portion estimate even achieves 33% the extent

of the obscured image. The obscure estimation issue can be decreased to a parameter estimation issue which is substantially more tractable. Parametric obscure estimation algorithms use the property that linear uniform obscure bit's range is sinc-like capacity which is unmistakable from characteristic image^[15]. In a current work, evaluated the ordinary vector of the plane in the camera scene and the camera's movement course to deal with the forward or in reverse movement obscure. For over-speed tag deblurring, the measure of obscure bit is extensive, notwithstanding achieving 33% of the span of obscured image, which postures extraordinary difficulties to both the MAP and underestimation techniques. To handle this issue, we embrace the obscure bit parameter estimation technique (point and length). For edge estimation, our plan influences utilization of the connection between the portion to point and meager portrayal coefficients. For length estimation, we misuse the way that the conduct of energy range is altogether influenced by the length of piece in Fourier domain. The real preferred standpoint of our strategy is that the proposed plan can deal with extensive movement obscure notwithstanding when the tag is unrecognizable by human, which makes our approach promising in genuine applications.

III. EVALUATION OF BLUR KERNEL

Generally, the blur kernel is determined by the relative motion between the moving vehicle and static surveillance

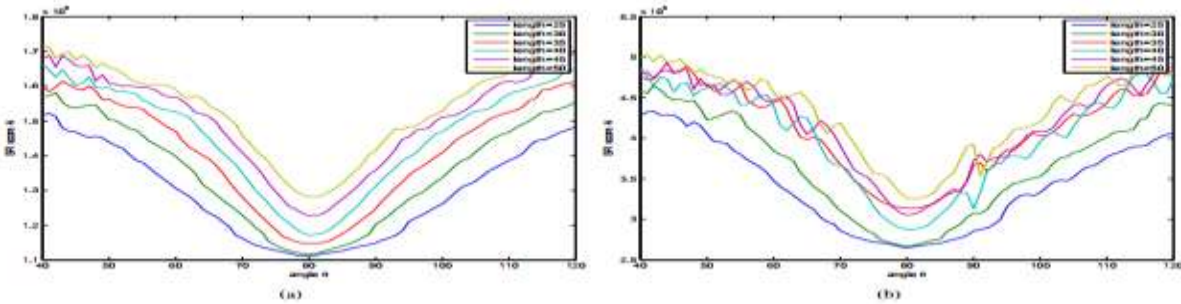


Fig:4 Relation between A and θ under different length settings, (a) Lena; (b) real license plate image. The ground truth setting is $(\theta = 80^\circ, l = 35)$.

camera amid the exposure time. At the point when the exposure time is short and the vehicle is moving quick, the movement can be viewed as linear and the speed can be considered as roughly consistent. In such cases, the obscure part of tag image can be demonstrated as a linear uniform bit with two parameters: point and length^[15].

where B is the obscured image, I means the dormant image to be recouped, $k\theta$ is the linear uniform movement portion controlled by edge θ (disregard length here), and $p(I)$ is the earlier of the sharp image. By presenting meager portrayal, in our edge estimation calculation, we endeavor to unravel:

$$\begin{aligned} \vartheta &= \underset{\Omega_i = D \alpha_i}{\operatorname{argmin}} \theta \sum |\alpha_i| \\ x &= \underset{\lambda}{\operatorname{argmin}} \{ \|I\|_{TV} + \frac{\lambda}{2} \|k\theta * I - B\|^2 \} \dots (3) \end{aligned}$$

where D is pre-learned over-total lexicon on the sharp tag images, Ω_i is the fix extraction administrator, and α_i is the inadequate portrayal coefficients of the i th fix. The physical significance of Eq. (4) is that the point we expect to gauge is the one with which the recouped sharp image has the sparsest portrayal^[16-19]. The way θ to unravel Eq. (4) is to assess the inclination however, it is hard to specifically illuminate such a two-layer optimization issue. Keeping in mind the end goal to explore the connection between $\sum |\alpha_i|$ and the variable θ , we break down Eq. (4) into two less difficult sub-issues. For a given parameter match (θ, l) , we initially take care of the accompanying optimization issue,

$$X = \underset{\lambda}{\operatorname{argmin}} \{ \|I\|_{TV} + \frac{\lambda}{2} \|k\theta * I - B\|^2 \} \dots (4)$$

Then the sparse representation coefficient $\sum |\alpha_i|$ can be computed by solving:

$$\begin{aligned} \operatorname{Min} & \alpha \sum |\alpha_i| \\ \Omega_i &= D \alpha_i \dots (5) \end{aligned}$$

Here, for straight forwardness, we characterize $A = \sum |\alpha_i|$. Consequently, $A(\theta, l)$ can be viewed as an element of portion parameters (θ, l) . With a specific end goal to investigate the property of $A(\theta)$ (overlook l here), we have done a few trials on two illustration images: Lena and a genuine sharp tag image (appeared in Fig. 3). Right off the bat, we obscure the sharp Lena and tag image with a linear uniform movement obscure bit with a point of 80 degrees and a length of 35 pixels $(\theta = 80^\circ, l = 35)$. The fundamental trouble in understanding the optimization by Eq. (4) is that the slope can't be ascertained productively. Be that as it may, the semi raised property from the inadequate portrayal expedites an incredible change this optimization issue. Despite the fact that the inclination $\partial A / \partial \theta$ has no shut frame, we can appraise the 0 10 20 30 40 50 60 70 80 90 0 2 4 6 8 10 12 14 16 18 20

Angle RMSE length=15 length=30 length=45 Fig.5 RMSE of point estimation. The commotion level is $\sigma = 5$. slope by registering Eq. (5) and (6) twice. At that point we utilize the angle plunge technique to discover the optimization esteem. In Fig. 4 and Fig. 5, we can see that there are a few anomalies on the bends. With a specific end goal to decrease the impact of exceptions, the progression of slope drop ought not be too little. In any case, substantial advance may prompt the corruption of precision. So we propose a two-advance coarse-to-fine point estimation calculation, which will be expounded on in Section III-C. The aftereffect of SURE in Fig.6 is acquired by Monte-Carlo calculation, in which each point is figured utilizing 10 cases. The SURE additionally demonstrates the comparative semi arched properties. In any case, the SURE keeps in low an incentive in expansive range around the ground truth (see blue, green and red bends in Fig.6 which makes it hard to decide the ideal point as the last estimation result. Not quite the same as the general regular scene images, tag images typically just contain some particular characters, for example, English letters and digits. Thusly, tag images are described by extremely specific and constrained examples, which can be all around learned by scanty portrayal. In this paper, our dictionary is prepared on sharp tag images. Consequently, the earlier information about tag images is as of now implanted in the over-total dictionary. In this

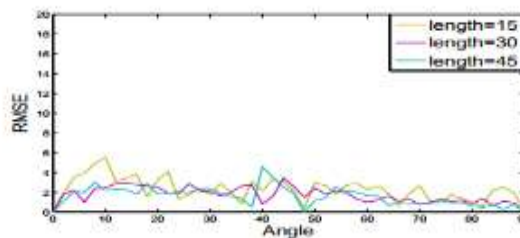


Fig:5 RMSE of angle estimation. The noiselevel is $\sigma = 5$.

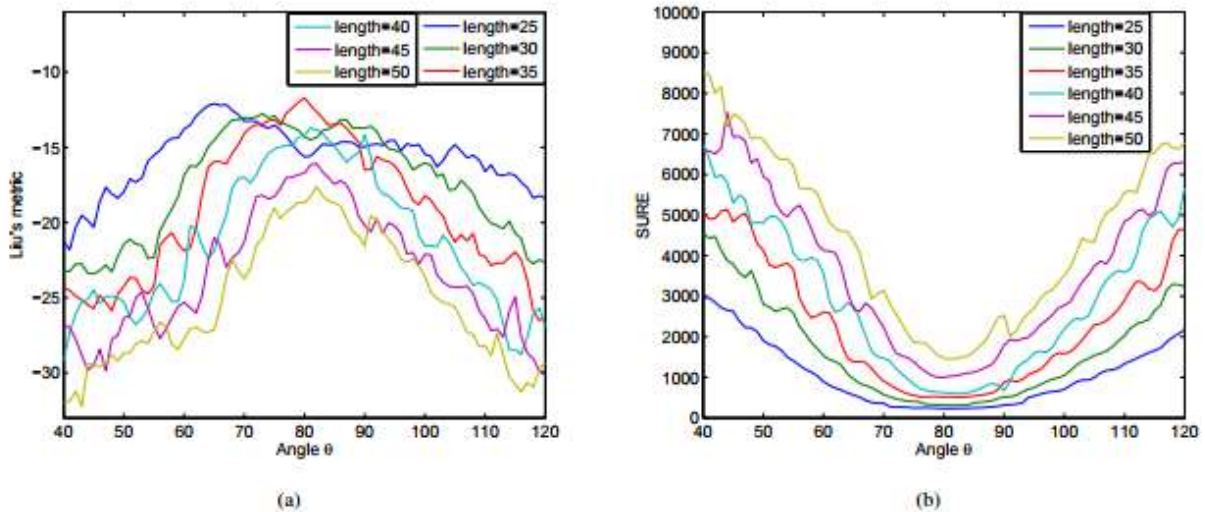


Fig:6 Performance of Liu's metric and SURE under different length settings for Fig. 3(b). (a) Liu's metric; (b) SURE obtained by Monte-Carlo algorithm. The ground truth setting is $(\theta = 80^\circ, l = 35)$.

As appeared in Fig.6 An accomplishes the base when l is set as 25, while the ground truth of length is 35. Besides, in Fig. 8, we plot the connection amongst Δn and l when the point is settled, where the inadequate portrayal coefficients demonstrate the monotonic expanding property with the expansion of l . At the end of the day, in the event that we utilize the sparsity on overcomplete dictionary and foras earlier, the outcome supports a shorter portion regardless of whether the edge is right or not.

3.1 Dimension evaluation of linear uniform kernel

Once the direction of motion has been fixed, we can rotate the blurred image to make this direction horizontal. Then the uniform linear motion blur.

The magnitude of the frequency response of $k(x, y)$ on horizontal direction is given by the following equation: here N is the size of blurred image in pixel. Given two successive zero points v_1, v_2 of $F_k(v)$, it is easy to obtain that:

$$L = \frac{N}{|v_1 - v_2|} \dots (6)$$

Thus, the core of length estimation is to estimate the distance between two adjacent zero points of frequency response of kernel. In frequency domain, the uniform blur model can be written as:

$$F_B(u, v) = F_K(u, v) F_I(u, v) + F_G(u, v) \dots (7)$$

where F indicates the Fourier change administrator. We can find that the zero purposes of Fk is likewise the zeros purposes of FB without thinking about commotion. In a large portion of genuine circumstances, it is hard to specifically look zero focuses in the frequency response of watched image. Because of commotion, the zero purposes of Fk may not precisely signify the zero purposes of FB; nonetheless, the extent of FB around zero focuses still can be recognized from different focuses as the power range of characteristic images along lines through the beginning point complies with the accompanying power law.

$$|F_{I(w)}| \propto |w|^{-\gamma} \dots (8)$$

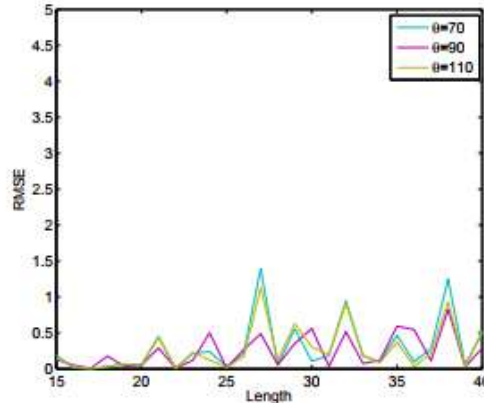


Fig:7 RMSE of length estimation.

where the estimation of γ may shift with the point of lines because of the nearness of expansive scale edge. Next, we abuse the powerlaw and Radon transform to deduce the separation between two nearby zero purposes of $|Fk|$. Radon transform is a necessary transform that gathers the entirety of a capacity over straight lines. Radon transform result can be spoken to by the edge between flat tomahawks α and the separation to the inception point ρ . For BID, Radon transform is proposed to evaluate the movement obscure piece, particularly when the watched image is defiled by commotion. In our length estimation calculation, we embrace the adjusted Radon transform which just considers the middle region of obscured image [16-18]. The adjusted random transform is characterized as:

where f is a general 2D function to be Radon transformed. For the blurred images, under weak noise assumption ($FG \approx 0$), we have

$$R_{\log|FB|}(\alpha, \rho) \approx R_{\log|F1|}(\alpha, \rho) + R_{\log|Fk|}(\alpha, \rho) \dots (9)$$

Based on the assumption of power-law, for one fixed angle α , $R_{\log|F1|}(\rho)$ is also a polynomial function. We use a three order polynomial function to fit $R_{\log|FB|}(\rho)$

$$R_{\log|FB|}(\rho) \approx (a\rho^3 + b\rho^2 + c\rho + d) \dots (10)$$

3.2 Summary of proposed scheme

In the point estimation organize, we receive a two-advance coarseto-fine structure. In the initial step, the semi raised property is used to locate the underlying best point under coarse granularity for any direct length. The calculation is abridged in Algorithm 1. When all is said in done, it just takes a few emphases for Algorithm 1 to merge. Once the underlying evaluated edge is gotten, we play out the fine point estimation. In Algorithm 1, every one of the tasks are connected on a settled length; while the fine estimation of edge is executed on a multi-length setting, the subtle elements of which can be found in Algorithm 2. In the two Algorithms 1 and 2, it is basic to unravel Eq. (5) and (6). The over-total dictionary D is pre-prepared on the sharp tag images. Both dictionary learning and Eq. (6) are settled with Lee's component sign calculation. For Eq. (5), there are numerous fruitful algorithms. In this paper, we embrace the mainstreapsplit-Bregmantangled earlier for the most part acquires high computational intricacy. The length estimation co.nspire is condensed in Algorithm 4 and its rule can be found in Section III-B. In the wake of getting the parameters of obscure part, the last nonblinddeblurring is finished with the NBID calculation proposed by Whyte et al. [19][20]

Algorithm 1 Coarse angle estimation

Input: Blurred image B , step Δ , initial angle θ_0 , a moderate length l , $k = 0$

- 1: **while** not converged **do**
- 2: Generate uniform linear kernel $k_{l,\theta_k}, k_{l,\theta_k-\Delta}, k_{l,\theta_k+\Delta}$
- 3: Solve Eq. (5) with kernels $k_{l,\theta_k}, k_{l,\theta_k-\Delta}, k_{l,\theta_k+\Delta}$, get deblurred images $I_{l,\theta_k}, I_{l,\theta_k-\Delta}, I_{l,\theta_k+\Delta}$
- 4: Solve Eq. (6) with $I_{l,\theta_k}, I_{l,\theta_k-\Delta}, I_{l,\theta_k+\Delta}$, get $A_{l,\theta_k}, A_{l,\theta_k-\Delta}, A_{l,\theta_k+\Delta}$
- 5: **if** $A_{l,\theta_k} == \min(A_{l,\theta_k}, A_{l,\theta_k-\Delta}, A_{l,\theta_k+\Delta})$
- 6: converged and return
- 7: **elseif** $A_{l,\theta_k-\Delta} == \min(A_{l,\theta_k}, A_{l,\theta_k-\Delta}, A_{l,\theta_k+\Delta})$
- 8: $\theta_k \leftarrow \theta_k - \Delta$
- 9: **else**
- 10: $\theta_k \leftarrow \theta_k + \Delta$
- 11: **end while**

Output: θ_k

Algorithm 2 Fine angle estimation

Input: Blurred image B , the output of Algorithm 1 θ , a moderate length l

- 1: Generate a series of pair (θ_i, l_i) (responding kernel k_i) that center about (θ, l)
- 2: Solve Eq. (5) with kernel k_i , get I_i
- 3: Solve Eq. (6) with I_i , get A_i
- 4: Sort A_i by increasing order
- 5: Get the top- k A_i and the corresponding θ_i

Output: The average of top- k θ_i

Algorithm 3 Non-blind image deblurring

Input: Blurred image B , kernel k , the balance parameter λ

- 1: Initialize the Bregman multipliers b_x, b_y and Bregman parameter r
- 2: **while** not converged **do**
- 3: $\arg\min_I \{ \frac{\lambda}{2} \|k * I - B\|_F^2 + \frac{\lambda}{2} \|d_x - \nabla_x I - b_x\|_F^2 + \frac{\lambda}{2} \|d_y - \nabla_y I - b_y\|_F^2 \}$, solved by gradient descent method
- 4: $\arg\min_{d_x} \{ \|d_x\| + \frac{\lambda}{2} \|d_x - \nabla_x I - b_x\|_F^2 \}$, solved by shrinkage operator
- 5: $\arg\min_{d_y} \{ \|d_y\| + \frac{\lambda}{2} \|d_y - \nabla_y I - b_y\|_F^2 \}$, solved by shrinkage operator
- 6: Update Bregman multiplier
- 7: $b_x \leftarrow b_x + \nabla_x I - d_x$
- 8: $b_y \leftarrow b_y + \nabla_y I - d_y$
- 9: **if** reach the max-iteration
- 10: converged and return
- 11: **endif**
- 12: **end while**

Output: The recovered image I

Algorithm 4 Length estimation

Input: Blurred image B , the output of Algorithm 2 θ

- 1: Extend B into a square image (the size is $N \times N$) and calculate logarithm of frequency magnitude of B denoted by $\log(|F_B|)$
- 2: Apply modified Radon transform on $\log(|F_B|)$ over the angle θ , $R_{\log(|F_B|)}(\rho)$ denotes the result
- 3: Fit $R_{\log(|F_B|)}(\rho)$ with three order polynomial function through least square error method, the fitting result is $\hat{R}_{\log(|F_B|)}(\rho)$
- 4: Get the distance of two consecutive local minimums of $R_{\log(|F_B|)}(\rho) - \hat{R}_{\log(|F_B|)}(\rho)$ denoted by d
- 5: Get the estimated length by $L = \frac{N}{d}$

Output: The length of kernel L

IV. EXPERIMENTAL RESULTS





Table:(1) Table For Recognition Rate Of Existing n Proposed Methods

BID Schemes	Recognition Rate
Unprocessed image	9.10%
NSBD [52]	18.18%
TPISD/USR [8], [10]	43.18%
Existing algorithm	79.55%
Proposed algorithm	94.96%

Table:(2) Table For Running Time Of Existing n Proposed Methods

BID schemes	Running time(s)
TPISD/USR(optimized by c++ and CUDA) [8],[10]	45.68
NSBD[52]	11.84
FSR[17]	135.23
HOMD(optimized by c++)[7]	736.89
Existing algorithm	347.95
Proposed algorithm	10.07

V.CONCLUSION

In this paper, a novel kernel parameter estimation calculation is proposed for license plate from quick moving vehicles. Under some extremely frail suppositions, the license plate deblurring issue can be decreased to a parameter estimation issue. A fascinating semi raised property of sparse representation coefficients with kernel parameter (point) is revealed and misused. This property drives to outline a coarse-to-fine calculation to appraise the edge positions, the license plate deblurring issue proficiently. The length estimation is finished by investigating the very much utilized power-range character of normal image. One preferred standpoint of this calculation is that model can deal with huge obscure kernel. As appeared by tests in Section IV, for the license plate that can't be perceived by human, the deblurred result winds up discernable. Another preferred standpoint

is that the plan is more robust. This advantages from the conservativeness of the model and also the way that technique does not make solid presumption about the substance of image, for example, edge or isotropic property.

In this plan, we just utilize extremely straightforward and credulous NBID calculation. What's more, there is as yet evident ancient rarity in the deblurred comes about. Be that as it may, for some viable applications, individuals are more intrigued by recognizing the semantics of the image. From this view, This plan expedites extraordinary change the license plate recognition.

REFERENCES

- [1] G. Adiv. Determining three-dimensional motion and structure from optical flow generated by several moving objects. *IEEE T. Pattern Anal. Mach. Intell.*, 7(4):384–401, July 1985. 3
- [2] S. Baker, D. Scharstein, J.P. Lewis, S. Roth, M. J. Black, and R. Szeliski. A database and evaluation methodology for optical flow. *Int. J. Comput. Vision*, 92(1):1–31, Mar. 2011. 6
- [3] A. Blake, C. Rother, M. Brown, P. Perez, and P. Torr. Interactive image segmentation using an adaptive GMMRF model. In *ECCV*, vol. 1, pp. 428–441, 2004.
- [4] W. Zhou, H. Li, R. Hong, Y. Lu, and Q. Tian, “Bsift: toward data independent codebook for large scale image search,” *IEEE Transactions on Image Processing (TIP)*, vol. 24, no. 3, pp. 967–979, 2015.
- [5] W. Zhou, M. Yang, H. Li, X. Wang, Y. Lin, and Q. Tian, “Towards codebook-free: Scalable cascaded hashing for mobile image search,” *IEEE Transactions on Multimedia (TMM)*, vol. 16, no. 3, pp. 601–611, 2014.
- [6] S. Cho and S. Lee, “Fast motion deblurring,” *ACM Transactions on Graphics (TOG)*, vol. 28, no. 5, pp. 145:1–145:8, Dec 2009.
- [7] Q. Shan, J. Jia, and A. Agarwala, “High-quality motion deblurring from a single image,” *ACM Transactions on Graphics (TOG)*, vol. 27, no. 3, pp. 73:1–73:10, 2008.
- [8] L. Xu, S. Zheng, and J. Jia, “Unnatural ℓ_0 sparse representation for natural image deblurring,” in *Proceedings of IEEE Conference on Computer Vision and Pattern Recognition (CVPR)*, Jun 2013, pp. 1107–1114.
- [9] approximation,” in *Proceedings of IEEE Conference on Computer Vision and Pattern Recognition (CVPR)*, Jun 2009, pp. 104–111.
- [10] A hybrid license plate extraction method based on edge statistics and morphology, BaiHongliang, Liu Changping Proceedings of the 17th International Conference, 2004.
- [11] H. Cho, J. Wang, and S. Lee, “Text image deblurring using text-specific properties,” in *Proceedings of European Conference on Computer Vision (ECCV)*, Oct 2012, pp. 524–537.
- [12] L. Xu and J. Jia, “Two-phase kernel estimation for robust motion deblurring,” in *Proceedings of European Conference on Computer Vision (ECCV)*, Sep 2010, pp. 157–170.
- [13] A. Levin, Y. Weiss, F. Durand, and W. T. Freeman, “Understanding blind deconvolution algorithms,” *IEEE Transactions on Pattern Analysis and Machine Intelligence (TPAMI)*, vol. 33, no. 12, pp. 2354–2367, 2011.
- [14] J. Oliveira, M. Figueiredo, and J. Bioucas-Dias, “Parametric blur estimation for blind restoration of natural images: linear motion and out-of-focus,” *IEEE Transactions on Image Processing (TIP)*, vol. 23, no. 1, pp. 466–477, Jan 2014.
- [15] R. Fergus, B. Singh, A. Hertzmann, S. T. Roweis, and W. T. Freeman, “Removing camera shake from a single photograph,” *ACM Transactions on Graphics (TOG)*, vol. 25, no. 3, pp. 787–794, 2006.
- [16] C. Wang, Y. Yue, F. Dong, Y. Tao, X. Ma, G. Clapworthy, H. Lin, and X. Ye, “Nonedge-specific adaptive scheme for highly robust blind motion deblurring of natural images,” *IEEE Transactions on Image Processing (TIP)*, vol. 22, no. 3, pp. 884–897, Mar 2013.
- [17] R. Hartley and A. Zisserman, *Multiple View Geometry in Computer Vision*, 2nd ed. Cambridge University Press, 2004.
- [18] J.-F. Cai, H. Ji, C. Liu, and Z. Shen, “Blind motion deblurring from a single image using sparse approximation,” in *Proceedings of IEEE Conference on Computer Vision and Pattern Recognition (CVPR)*, Jun 2009, pp. 104–111.

[19] W. Zuo, D. Ren, D. Zhang, S. Gu, and L. Zhang, "Learning iterationwise generalized shrinkage-thresholding operators for blind deconvolution," IEEE Transactions on Image Processing, vol. 25, no. 4, pp. 1751–1764, April 2016.

[20] L. Xu and J. Jia, "Two-phase kernel estimation for robust motion deblurring," in ECCV, 2010, pp. 157–170.

